Proceedings of the 42th "Jaszowiec" International School and Conference on the Physics of Semiconductors, Wisła 2013

X-Ray Photoelectron Spectroscopy Study of Nitrogen and Aluminum–Nitrogen Doped ZnO Films

A. Ievtushenko[a,*], O. Khyzhun[a], I. Shtepliuk[a], V. Tkach[b], V. Lazorenko[a] and G. Lashkarev[a]

[a]I. Frantsevich Institute for Problems of Material Science, National Academy of Science of Ukraine, Kyiv, Ukraine
[b]V. Bakul Institute for Superhard Materials, National Academy of Science of Ukraine, Kyiv, Ukraine

Undoped, nitrogen-doped and aluminum–nitrogen co-doped ZnO films were deposited on Si substrates by magnetron sputtering using layer-by-layer method of growth. X-ray photoelectron spectroscopy was employed to characterize electronic properties of undoped and nitrogen doped ZnO films. The effects of N and N–Al incorporation into the ZnO matrix on the X-ray photoelectron spectroscopy core-level and valence-band spectra of the films were studied and discussed.

DOI: 10.12693/APhysPolA.124.858
PACS: 79.60.−i, 77.55.hf, 68.55.Ln

1. Introduction

ZnO has been intensively investigated as a promising material for optoelectronic devices because of its wide-band gap of about 3.3 eV and large exciton binding energy (60 meV) at room temperature [1] as well as ecological and economic benefits in comparison with GaN [2]. The modification of the physical properties of ZnO by doping will help to solve the problem of control of donor-type defects influencing the stability of properties of ZnO-based devices [3]. Nitrogen doping and aluminum–nitrogen co-doping of ZnO was used in order to obtain the p-type conductivity [4], increase the solubility of nitrogen in ZnO lattice [5] and improve the photovoltaic properties of different types of ZnO-based detectors of UV radiation as discussed in detail in Refs. [6–8].

However, nitrogen-doping and aluminum–nitrogen co-doping ZnO films should cause some changes of the energy distribution of the electronic states within the valence-band region of the obtained films as well as altering values of binding energies of the X-ray photoelectron spectroscopy (XPS) core-levels associated with zinc and oxygen atoms. To the best of our knowledge, such doping and co-doping effects have not been studied in detail so far. To fill this gap, in this paper we report on XPS studies of the effect of nitrogen doping and aluminum–nitrogen co-doping upon the electronic structure of ZnO films.

2. Experimental details

N-doped and Al–N co-doped ZnO films were grown on Si(100) substrates by radio-frequency (rf) magnetron sputtering using zinc and zinc-aluminum metallic targets by using the layer-by-layer growth method [9–11]. Nitrogen doping was performed during the ZnO films growth by addition in the deposition chamber to oxygen–argon working gas mixture of nitrogen (N_2) with pressure of 0.1 to 0.3 Pa. The rf discharge power was maintained at 200 W. The pressure of oxygen and argon was about 0.7 and 1.0 Pa, respectively. The substrate temperature was fixed at 400 °C. The target–substrate distance was approximately 7 cm, and the deposition time was 1 h.

The technique of the present XPS measurements was similar to that described in detail in Refs. [12, 13]. Briefly, acquisition of XPS valence-band and core-level spectra was carried out in a sublimation ion-pumped chamber having a base pressure less than 5×10^{-10} mbar of the UHV-Analysis System (SPECS, Germany) equipped with a PHOIBOS 150 hemispherical energy analyzer. The energy scale of the spectrometer was calibrated by setting the measured Au $4f_{7/2}$ and Cu $2p_{3/2}$ binding energies (BEs) to 84.00 ± 0.05 eV and 932.66 ± 0.05 eV, respectively, with regard to the Fermi energy, E_{F}. The XPS spectra were excited by a Mg K_α source of X-ray radiation ($E = 1253.6$ eV) and were recorded at a constant pass energy of 25 eV. The charging effects were taken into account in reference to the C 1s line (285.0 eV) of adventitious carbon. The elemental analysis of ZnO:N films was done by a ZEISS EVO 50 XVP SEM apparatus using energy dispersive X-ray spectroscopy (EDX) furnished INCA 450 (OXFORD Instruments).

3. Results and discussion

Using the EDX spectroscopy the concentration of nitrogen and aluminum in ZnO films was defined. Concentration of aluminum in the N–Al co-doped ZnO film was found to be approximately 0.24 wt%. The nitrogen concentrations in ZnO films will be reported below.

N doped and N–Al co-doped ZnO films possess n-type conductivity. It is confirmed by thermoelectric studies of

*corresponding author; e-mail: a.ievtushenko@yahoo.com

the samples. It should be noted that the doping of ZnO by the above-mentioned additives did not lead to change of the conductivity type in ZnO. This finding is invoked by self-compensation effect at acceptor doping [14].

The effect of incorporation of nitrogen and nitrogen with aluminum into the ZnO lattice during film growth on peculiarities of its chemical bonding and the electronic structure has been investigated in the present work by measuring the XPS core-level and valence-band spectra of the films under study. As can be seen from Fig. 1, the intensive lines of O 1s ($\approx$ 530.5 eV), Zn $2p_{3/2}$ and Zn $2p_{1/2}$ (lines with binding energies of 1021 and 1044 eV, respectively) are observed on the survey XPS spectra of all the films studied. Binding energies of these lines correspond to those of the similar XPS core levels of matrix elements of ZnO wurtzite structure [15]. A weak line positioned at 72.6 eV (spectrum 3 in Fig. 1) corresponds to the 2p states of Al in the ZnO:N,Al film. No peak at 74.3 eV in the spectrum of the ZnO:N,Al film (spectrum 3 in Fig. 1) that is related to the 2p state of Al in Al_2O_3 was observed. This fact may confirm our suggestion that Al substitutes Zn in the cation sublattice of ZnO when the ZnO:N,Al film is formed.

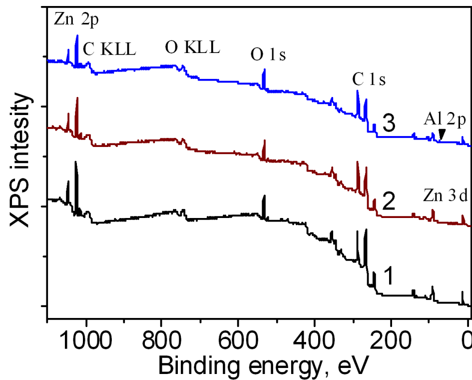

Fig. 1. Survey XPS spectra of (1) undoped ZnO, (2) nitrogen doped ZnO (ZnO:N, $C_{\rm N}$ = 0.70 wt%), and (3) nitrogen–aluminum co-doped zinc oxide (ZnO:N, Al; $C_{\rm N}$ = 1.1 wt%) films.

XPS spectra of nitrogen-doped ZnO films are characterized by the presence of weak N 1s lines located in the energy range of 395–415 eV (Fig. 2). In this energy range, there are two components of the N 1s spectra, which can be caused by the existence of two different chemical bonds of nitrogen atoms with the surrounding atoms. The low-energy component of the XPS N 1s core-level spectra with binding energy of about 398.3 eV is caused by the formation of chemical N–Zn bonds arising from the substitution of oxygen atoms by nitrogen atoms in the nitrogen doped ZnO film [16]. The appearance of the high-energy component of the XPS N 1s core-level spectra with binding energy of about 408.4 eV is due to the presence of chemical N–O bonds, which can be caused by nitrogen atoms adsorbed on the oxide surface [17, 18]. Thus, the presence of the low-energy component of the XPS N 1s core-level spectra with binding energy $\approx$ 398.3 eV confirms the occurrence of acceptor additive nitrogen in the case of doping with nitrogen only (curve 1 in Fig. 2), and in the case of its entry into the lattice of ZnO with aluminum (curve 2 in Fig. 2).

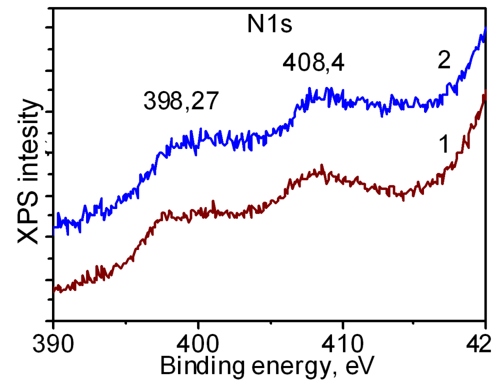

Fig. 2. XPS N 1s core-level spectra of (1) nitrogen doped ZnO (ZnO:N, $C_{\rm N}$ = 0.70 wt%) and (2) nitrogen–aluminum co-doped zinc oxide (ZnO:N, Al; $C_{\rm N}$ = 1.1 wt%) films.

Figure 3 shows the XPS O 1s core-level spectra of the undoped ZnO as well as for nitrogen doped and nitrogen–aluminum co-doped zinc oxide films. The asymmetric shape of the XPS O 1s spectra and the presence of two fine-structure features indicates that oxygen exists in the ZnO films in two chemical states associated with surface O–Zn and O–N chemical bonds [19]. The approximation of XPS O 1s spectra by Gaussian function into two components allows making a detailed analysis of the impact of the introduction of nitrogen in the zinc oxide lattice on the chemical state of oxygen. As a result, it was found that the O 1s spectrum consists of two components positioned at 530.08 $\pm$ 0.05 eV and 532.02 $\pm$ 0.05 eV. The first component corresponds to oxygen involved in the formation of O–Zn bonds [20]. The relative intensity of the second component of the XPS O 1s core-level spectra is proportional to the oxygen vacancies ($V_{\rm O}$) concentration in ZnO [21].

The changes of the surface chemical bonding and electronic properties of ZnO caused by nitrogen incorporation into lattice can be estimated by calculating the relative proportion of each component (RPC_i) [22]:

$$\mathrm{RPC}_i = \frac{I_i}{I_{\rm p}}, \tag{1}$$

where I_i is integrated intensity of i-th component, $I_{\rm p}$ is integrated intensity of peak, which is decomposed into components.

Results of deconvolution of the O 1s spectra on the components caused by different states of oxygen and calculated using (1) are shown in Fig. 4. The relative percentage of the component ascribed to O–Zn bonds in the surface layers of undoped ZnO is 32%. The relative percentage of the component associated with the O^{2-} ions

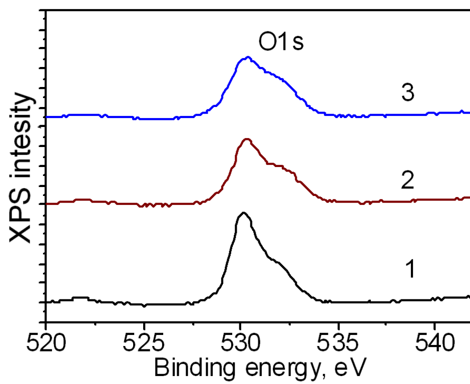

Fig. 3. XPS O 1*s* core-level spectra of (1) undoped ZnO, (2) nitrogen doped ZnO (ZnO:N, C_{N} = 0.70 wt%), and (3) nitrogen–aluminum co-doped zinc oxide (ZnO:N, Al; C_{N} = 1.1 wt%) films.

in the oxygen-deficient regions within the matrix of ZnO is 68%. The relative intensities of these peaks are partly related to the variation in the concentration of oxygen vacancies (that can be filled by nitrogen) on the surface of the ZnO films (Fig. 4). With increasing nitrogen concentration in the ZnO lattice the redistribution of chemical bonds is observed. Relative percentage of the component related to the O–Zn bonds is increased by 23% for the N-doped and N–Al co-doped ZnO films. Simultaneously, the percentage of the component associated with oxygen vacancies concentration is decreased. Therefore nitrogen doping and aluminum–nitrogen co-doping of the ZnO films lead to decreasing concentration of oxygen vacancies in the surface layers (reduced RPC_i, which is responsible for oxygen vacancies).

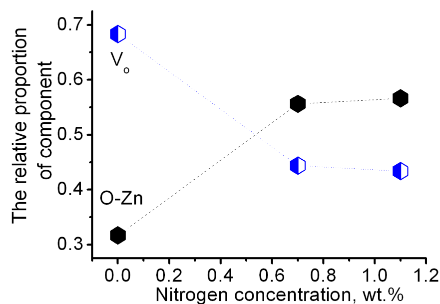

Fig. 4. Results of analysis of the XPS O 1*s* core-level spectrum components for the undoped ZnO as well as for nitrogen doped and nitrogen–aluminum co-doped zinc oxide films.

Figure 5 presents the XPS Zn 2*p* core-level spectra of the undoped ZnO and nitrogen doped and nitrogen–aluminum co-doped zinc oxide films. The XPS Zn 2*p* spectra are simple spin–orbit doublets formed by the Zn $2p_{3/3}$ and Zn $2p_{1/2}$ electrons with binding energies of 1021.72 ± 0.05 eV and 1044.79 ± 0.05 eV, respectively. Symmetrical form of the Zn 2*p* spectra and their small half-width values (1.81 ± 0.05 eV) indicate that Zn^{2+} ions are in a tetrahedral oxygen environment and the chemical Zn–O bonds are dominant in the films studied. However, it should be noted that the integrated area of the XPS spectra of Zn $2p_{3/2}$ core-level electrons decreases after nitrogen doping of ZnO, indicating a decrease of the portion of the chemical Zn–O bonds, that is obviously due to nitrogen incorporation into ZnO lattice.

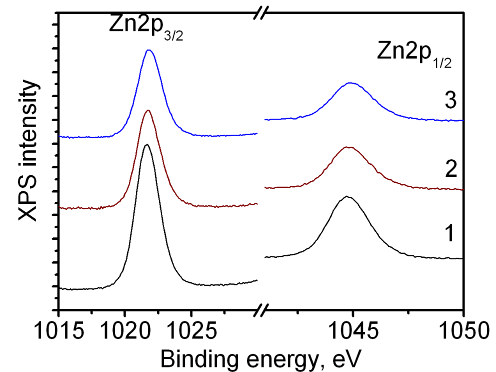

Fig. 5. XPS Zn 2*p* core-level spectra of (1) undoped ZnO, (2) nitrogen doped ZnO (ZnO:N, C_{N} = 0.70 wt%), and (3) nitrogen–aluminum co-doped zinc oxide (ZnO:N, Al; C_{N} = 1.1 wt%) films.

XPS valence band spectra of undoped and nitrogen--doped ZnO films consist of three peaks, which are marked as A, B and C features in Fig. 6. The feature in the energy range of 2–8 eV below the Fermi level (feature A) is formed by the O 2*p* states hybridizing with the Zn 4*s* and Zn 4*p* states. The peak at ≈ 11 eV (feature B) is ascribed to the 3*d* states of zinc, whereas the feature C (≈ 23 eV below the Fermi level) is formed by the 2*s* states of oxygen [15].

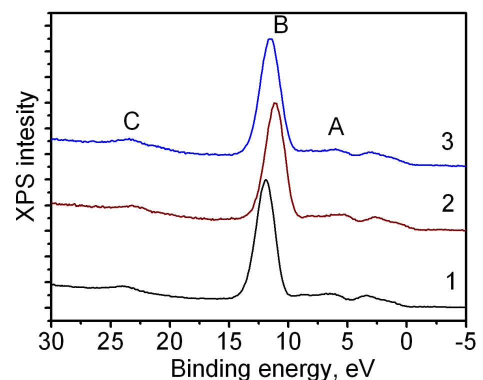

Fig. 6. XPS valence-band spectra of (1) undoped ZnO, (2) nitrogen doped ZnO (ZnO:N, C_{N} = 0.70 wt%), and (3) nitrogen–aluminum co-doped zinc oxide (ZnO:N, Al; C_{N} = 1.1 wt%) films.

In the case of undoped ZnO the maximum of the peak formed by the Zn 3*d* states is located at 11.94 eV. Doping

ZnO by nitrogen leads to a significant increase in half--width of the peak and causes it to shift towards lower binding energies. In the binding energy range of 4–6 eV, the uppermost valence-band edges (VBE) could be easily separated out. The position of the valence band maximum (VBM) can be evaluated by taking a linear extrapolation of the onset of the XPS valence band spectra. The tangent to the fitted curve was drawn and intersect is defined as the VBM. The binding energy shift in the VBM with respect to the Fermi level, E_F, was obtained. For undoped ZnO the position of the Fermi level is 3.14 eV that is close to the bottom of the conduction band. This position of the Fermi level determines the n-type conductivity due to the deviation from the stoichiometric composition of undoped ZnO. By increasing the concentration of nitrogen in ZnO from 0.70 to 1.1 wt%, the position of the Fermi level is lowered from 2.54 eV to 2.11 eV, respectively. This shift of the Fermi level position compared to that of the undoped zinc oxide (3.14 eV) is associated with an increase in the concentration of acceptor additives of nitrogen and formation of the Zn–N chemical bonds corresponding to the introduction of nitrogen ions into the oxygen sublattice.

4. Conclusions

In summary, data of X-ray photoelectron spectroscopy together with comprehensive analysis of structure and stoichiometry demonstrate that nitrogen incorporates into ZnO lattice after both N doping and N–Al co-doping. It has been found that in the both cases nitrogen ions substitute the oxygen ones in anion sublattice and cause the shift of the Fermi level toward the valence band maximum. Doping ZnO by nitrogen leads to a decrease in the concentration of donor defects (oxygen vacancies) that can play a rather positive role for development of high efficient ZnO-based detectors of ultraviolet irradiation.

References

[1] G.V. Lashkarev, V.A. Karpyna, V.I. Lazorenko, A.I. Ievtushenko, I.I. Shtepliuk, V.D. Khranovskyy, *Low Temp. Phys.* **37**, 226 (2011).

[2] V.A. Karpina, V.I. Lazorenko, C.V. Lashkarev, V.D. Dobrowolski, L.I. Kopylova, V.A. Baturin, S.A. Pustovoytov, A. Ju. Karpenko, S.A. Eremin, P.M. Lytvyn, V.P. Ovsyannikov, E.A. Mazurenko, *Cryst. Res. Technol.* **39**, 980 (2004).

[3] J.-H. Kang, D.W. Kim, J.H. Kim, Y.S. Lim, M.-H. Lee, W.-S. Seo, H.J. Choi, K.H. Seo, M.G. Park, *Thin Solid Films* **519**, 6840 (2011).

[4] H. von Wenckstern, H. Schmidt, M. Brandt, A. Lajn, R. Pickenhain, M. Lorenz, M. Grundmann, D.M. Hofmann, A. Polity, B.K. Meyer, H. Saal, M. Binnewies, A. Börger, K.-D. Becker, V.A. Tikhomirov, K. Jug, *Prog. Solid State Chem.* **37**, 153 (2009).

[5] T. Yamamoto, H. Katayama-Yoshida, *J. Cryst. Growth* **214/215**, 552 (2000).

[6] A.I. Ievtushenko, G.V. Lashkarev, V.I. Lazorenko, V.A. Karpyna, M.G. Dusheyko, V.M. Tkach, L.A. Kosyachenko, V.M. Sklyarchuk, O.F. Sklyarchuk, K.A. Avramenko, V.V. Strelchuk, Zs.J. Horvath, *Phys. Status Solidi A* **207**, 1746 (2010).

[7] L.A. Kosyachenko, G.V. Lashkarev, V.M. Sklyarchuk, A.I. Ievtushenko, O.F. Sklyarchuk, V.I. Lazorenko, A. Ulyashin, *Phys. Status Solidi A* **207**, 1972 (2010).

[8] L.A. Kosyachenko, G.V. Lashkarev, A.I. Ievtushenko, V.I. Lazorenko, V.M. Sklyarchuk, O.F. Sklyarchuk, *Acta Phys. Pol. A* **119**, 681 (2011).

[9] A.I. Ievtushenko, G.V. Lashkaryov, V.V. Strelchuk, V.I. Lazorenko, L.O. Klochkov, O.S. Lytvyn, V.M. Tkach, A.S. Romanyuk, K.A. Avramenko, O.I. Bykov, V.A. Baturin, A.Y. Karpenko, *Metallofiz. Nov. Tekhnol.* **33**, 243 (2011).

[10] A. Ievtushenko, V. Karpyna, G. Lashkarev, V. Lazorenko, V. Baturin, A. Karpenko, M. Lunika, A. Dan'ko, *Acta Phys. Pol. A* **114**, 1131 (2008).

[11] A.I. Ievtushenko, V.A. Karpyna, V.I. Lazorenko, G.V. Lashkarev, V.D. Khranovskyy, V.A. Baturin, O.Y. Karpenko, M.M. Lunika, K.A. Avramenko, V.V. Strelchuk, O.M. Kutsay, *Thin Solid Films* **518**, 4529 (2010).

[12] I. Shtepliuk, G. Lashkarev, O. Khyzhun, B. Kowalski, A. Reszka, V. Khomyak, V. Lazorenko, I. Timofeeva, *Acta Phys. Pol. A* **120**, 914 (2011).

[13] I. Shtepliuk, O. Khyzhun, G. Lashkarev, V. Khomyak, V. Lazorenko, I. Timofeeva, *Acta Phys. Pol. A* **122**, 1034 (2012).

[14] Y. Liu, H.-J. Jin, C.-B. Park, G.C. Hoang, *Trans. Electric. Electron. Mater.* **10**, 24 (2009).

[15] J. Moulder, W.F. Stickle, P.E. Sobol, K.D. Bomben, J. Chastain, *Handbook of X-ray Electron Spectroscopy*, Perkin-Elmer, Minnesota 1992.

[16] M. Petravic, P.N.K. Deenapanray, V.A. Coleman, C. Jagadish, K.-J. Kim, B. Kim, S. Koike, M. Sasa, M. Inoue, M. Yano, *Surf. Sci.* **600**, L81 (2006).

[17] J.M. Bian, X.M. Li, X.D. Gao, W.D. Yu, L.D. Chen, *Appl. Phys. Lett.* **84**, 541 (2004).

[18] Y.-J. Zeng, Z. Zh. Ye, J.-G. Lu, L.-P. Zhu, D.-Y. Li, B.-H. Zhao, J.-Y. Huang, *Appl. Surf. Sci.* **249**, 203 (2005).

[19] N. Tabet, M. Faiz, A. Al-Oteibi, *Electron Spectrosc. Relat. Phenom.* **163**, 15 (2008).

[20] M. Chen, X. Wang, Y.H. Yu, Z.L. Pei, X.D. Bai, C. Sun, R.F. Huang, L.S. Wen, *Appl. Surf. Sci.* **158**, 134 (2000).

[21] S.-M. Park, T. Ikegami, K. Ebihara, *Thin Solid Films* **513**, 90 (2006).

[22] L. Li, L. Fang, X.J. Zhou, Z.Y. Liu, L. Zhao, Sh. Jiang, *Electron Spectrosc. Relat. Phenom.* **173**, 7 (2009).